A Bilateral Lightwave Network Analyzer—Architecture and Calibration

Balasundaram Elamaran, *Member, IEEE*, Roger D. Pollard, *Fellow, IEEE*, and Stavros Iezekiel, *Senior Member, IEEE*

***Abstract*—The first bilateral lightwave network analyzer (BLNA) architecture that is capable of two-port S-parameter measurements is reported in this paper. A combined two-tier calibration is proposed and implemented for electrooptic and optoelectronic measurements. Calibrated measurement results showing the good performance of the BLNA for all types of lightwave components are also presented.**

***Index Terms*—Microwave measurements, optical variables measurement.**

I. Introduction

THE continuing growth in the application of lightwave techniques to microwave systems (such as fiber-optic communications [1], fiber-radio picocells [2], optical beamforming in phased-array antennas [3], all-optical microwave filters [4], and optical control of microwave components [5]) has created new challenges for microwave metrology. A microwave fiber-optic link, for example, will employ a diverse range of two-ports, which come under the umbrella term of lightwave components. These are classified into four categories depending on whether the signal at the input and output ports is electrical (E) or optical.

Lightwave network analysis is defined as the measurement of the small-signal microwave characteristics (such as modulation frequency response, transmission gain/loss, return loss, and phase delay) of electrical (E/E), electrooptic (E/O), optoelectronic (O/E) and optical (O/O) two-ports. Although characterization of E/E components is readily carried out with automated microwave vector network analyzers, for which a wealth of two-port calibration techniques is available [6]–[8], corresponding measurement techniques for E/O, O/E, and O/O two-port parameters are less developed. For example, the industry-standard lightwave network analyzer [9] requires two measurement configurations and up to four distinct calibrations to measure all four types of lightwave components. Moreover, the lightwave calibrations are simple normalization procedures, which can lead to error-prone measurements. In this respect, contemporary lightwave test sets and calibration of them have not progressed much beyond the work described in [10] and [11].

Manuscript received March 2, 2000; revised September 18, 2000. This work was supported by Agilent Technologies (formerly Hewlett-Packard Company), Santa Rosa, CA. The work of B. Elamaran was supported under a U.K. Overseas Research Scholarship and by the IEEE Microwave Theory and Techniques Society under a Graduate Fellowship.

The authors are with the Institute of Microwaves and Photonics, School of Electronic and Electrical Engineering, The University of Leeds, Leeds LS2 9JT U.K. (e-mail: b.elamaran@ieee.org).

Publisher Item Identifier S 0018-9480(00)10739-2.

One proposal aimed at overcoming the unilateral nature of prior test sets made use of bilateral E/O networks in a cascade arrangement, which potentially allows application of thru-refelction-line (TRL)-type calibrations to lightwave components [12]. Despite the conceptual elegance, the method has only been demonstrated for one-port measurement of O/O devices [13]. Other recent developments in the field include the development of two-port test sets and self-calibrations for O/O components [14]–[16]. These echo microwave vector-network analyzers, in that the test sets are bilateral. That is, a single connection of the O/O device-under-test (DUT) is made to the test set, and all four modulation S-parameters can be measured with a single configuration. We have previously presented some results that demonstrate the feasibility of an E/O network analyzer [17]. However, a complete bilateral lightwave network analyzer (BLNA) has yet to be demonstrated that would offer the same features for *all* lightwave two-ports.

This paper describes an automated BLNA that is capable of measuring two-port S-parameters of any lightwave component with a single connection of the DUT to the test set. This is facilitated by the use of microwave and optical double reflectometers together with microwave and optical signal switching. The BLNA offers a number of advantages. Firstly, the bilateral test set means the number of connect-disconnect cycles (and, hence, operator steps) is reduced compared to conventional analyzers [9]. Secondly, two-port self-calibration techniques can be applied to E/E and O/O measurements, and the latter can also be used as the first stage in E/O and O/E calibrations. The following sections describe the architecture of the BLNA, the associated full two-port lightwave calibration techniques, and measurement results.

II. BLNA: Architecture

The prototype BLNA was constructed from an HP 8510C microwave test set module, a microwave switch, a laser emitting at a wavelength of 1.3 μm, two amplified and one unamplified lightwave receivers, and two lightwave directional couplers. In addition, an external computer was used to control the BLNA and conduct calibration procedures and measurements. The block diagram of the BLNA is shown in Fig. 1. Incident and reflected microwave signals are denoted by a_i^{E} and b_i^{E}, while a_i^{OM} and b_i^{OM} are the corresponding optical variables. The waves following the power-combiner module originate from either the microwave or the optical test set, hence, the subscript R (resultant) is used to differentiate them from those of the microwave test set itself.

At the heart of the BLNA are the microwave and optical test sets shown in Figs. 2 and 3, respectively. A microwave signal

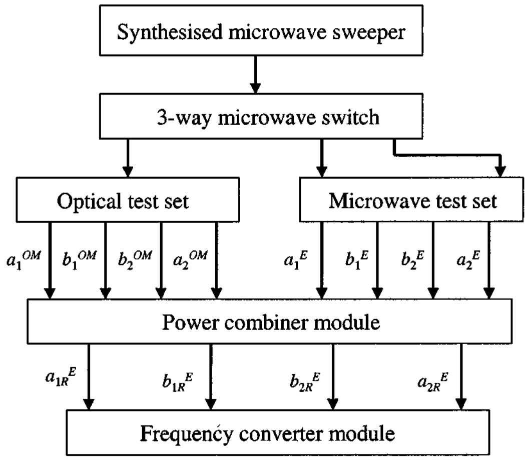

Fig. 1. Block diagram of BLNA concept.

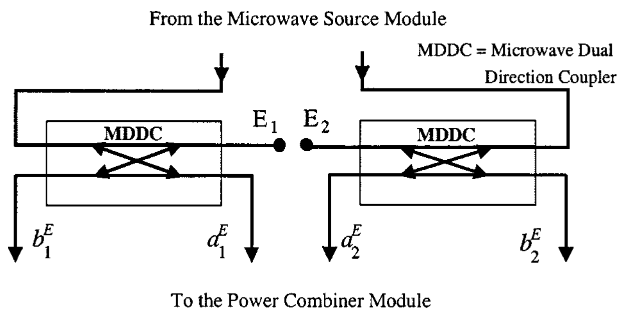

Fig. 2. Microwave test set of BLNA.

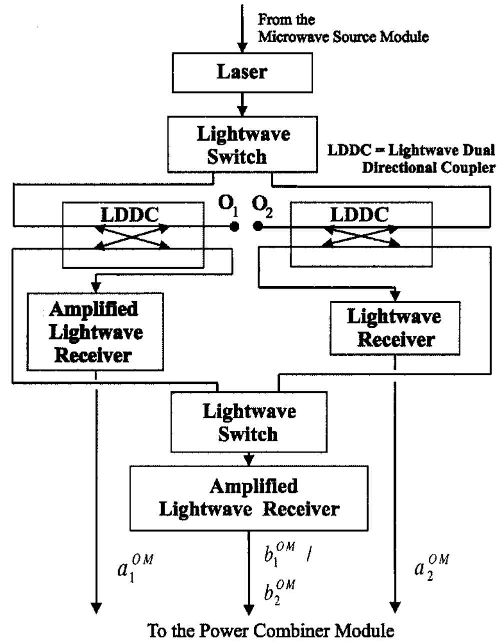

Fig. 3. Optical test set of the BLNA.

from a synthesized sweeper is directed into the test sets by a three-way microwave switch. Two switch positions are allocated for the microwave test set in order to supply microwave ports 1 and 2, respectively. Incident and reflected waves at the appropriate ports are then separated by the microwave dual directional couplers (Fig. 2) and passed to the power-combiner module for subsequent detection in the frequency converter module. However, only one route is required for the optical test set (Fig. 3), with the microwave signal directly modulating the laser diode, the output of which is then branched out via a lightwave switch to optical ports 1 and 2. The resulting incident and reflected lightwaves are separated by lightwave dual directional couplers, detected by three lightwave receivers, and passed onto the power-combiner module. Errors introduced by the couplers are quantified by the directivity error. Similarly, the switches in the source path lead to additional errors in the measurements, although uncertainty limits can be specified. The switch error (after calibration) falls mainly under the load match error term.

The prototype employed two amplified and one unamplified lightwave receivers. With the unamplified receiver being used to detect b_1^{OM} or b_2^{OM}, a reduced dynamic range for subsequent measurements is observed. Although external power amplifiers might be used, they are unable to detect small power levels from the photodiodes without also increasing noise content. Hence, an unamplified receiver was used to detect a_2^{OM}, one amplified receiver to detect a_1^{OM}, and another was switched between b_1^{OM} and b_2^{OM}. This arrangement was a cost-effective way to realize the prototype, although it is clear that improved performance could be achieved by employing amplified lightwave receivers throughout.

Similar signals from the optical and microwave test sets (e.g., $-a_1^{\mathrm{E}}$ and a_1^{OM}) are combined using three power combiners (Fig. 4) before being passed to the frequency converter module, where they are down converted and sampled for further processing. The use of power combiners makes it possible to use a simple four-channel frequency converter; otherwise eight channels would be required with only four in use for any one measurement. The power combiners are, therefore, an important part of the BLNA in terms of efficient use of components.

III. Measurement Procedures

The ports to which the four types of lightwave components should be connected are listed in Table I along with the corresponding measured quantities resulting from the switch settings. Both E/O and O/E DUTs are connected between the same ports, the only difference being that the forward configuration for the E/O measurements is the reverse of that for the O/E DUT measurements. The use of power combiners requires that neither ports E_1 and O_1, nor ports E_2 and O_2 are simultaneously used because signals from these ports share the same combiners; it is evident from the table that the measurement configurations satisfy these requirements.

The connection of E/O and O/E components between the same ports paves the way for the possible implementation of a single two-port calibration for both sets of measurements. The only calibrations demonstrated prior to this paper for E/O and O/E measurements are simple normalization calibrations, and two separate calibrations are required, one for each type. Although a two-port calibration using a bilateral electrooptic net-

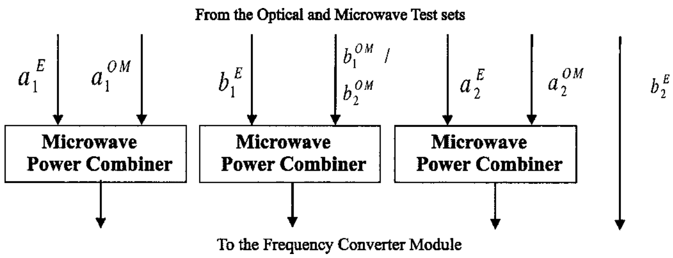

Fig. 4. Power-combiner module of the BLNA.

TABLE I
MEASUREMENT CONFIGURATION AND THE CORRESPONDING MEASURED QUANTITIES OF THE DUT MEASUREMENTS OF THE FOUR TYPES OF LIGHTWAVE COMPONENTS

DUT Type	BLNA Port Connection of DUT		Measured Quantities			
	Port 1	Port 2	$a_{1R}^E=$	$b_{1R}^E=$	$a_{2R}^E=$	$b_{2R}^E=$
E/E	E_1	E_2	a_1^E	b_1^E	a_2^E	b_2^E
E/O	E_1	O_2	a_1^E	b_1^E	a_2^{OM}	b_2^{OM}
O/E	O_2	E_1	a_2^{OM}	b_2^{OM}	a_1^E	b_1^E
O/O	O_1	O_2	a_1^{OM}	b_1^{OM}	a_2^{OM}	b_2^{OM}

work (BEON) was suggested in [12], it was validated neither by simulations, nor experiments. In addition, it may be argued that the theory is limited in that the effect of the BEON is not removed from the normalized error network and could result in subsequent measurement results being scaled. Since the work of [12], a generalized $\mathrm{T}xy$ calibration procedure has been developed in the microwave domain [8]. This forms the basis of a two-tier combined E/O and O/E calibration, in which the generalized $\mathrm{T}xy$ procedure is implemented as the first tier, and a deembedding procedure is used as the second tier to remove the effect of the BEON [17].

IV. COMBINED E/O AND O/E TWO-TIER CALIBRATION

The generalized $\mathrm{T}xy$ calibration procedure requires three two-port or double one-port standards. A thru must be chosen as the first standard, while the second standard must have zero reflections. However, the lack of critical components, specifically E/O or O/E thrus and reciprocal reflectionless standards, prevents the direct application of this calibration procedure for E/O and O/E measurements.

These limitations can be overcome by applying a two-tier calibration approach [17]. In the first-tier, the microwave test port E_1 is transformed into an optical port O_1' by using a BEON [13] (Fig. 5). An optical $\mathrm{T}xy$ calibration is then applied between ports O_1' and O_2.

The three measurements obtained from the optical calibration standards in cascade with the BEON can be expressed using the notation in [8] as

$$\mathbf{M}_1 = \mathbf{A}\mathbf{T}_{\mathrm{BEON}}^{\mathrm{EO}}\mathbf{N}_1^{\mathrm{OO}}\mathbf{B}^{-1} \tag{1}$$

$$\mathbf{M}_2' = m_{2x}\mathbf{A}\mathbf{T}_{\mathrm{BEON}}^{\mathrm{EO}}\mathbf{N}_2^{\mathrm{OO}}\mathbf{B}^{-1} \tag{2}$$

and

$$\mathbf{M}_3' = m_{3x}\mathbf{A}\mathbf{T}_{\mathrm{BEON}}^{\mathrm{EO}}\mathbf{N}_3^{\mathrm{OO}}\mathbf{B}^{-1} \tag{3}$$

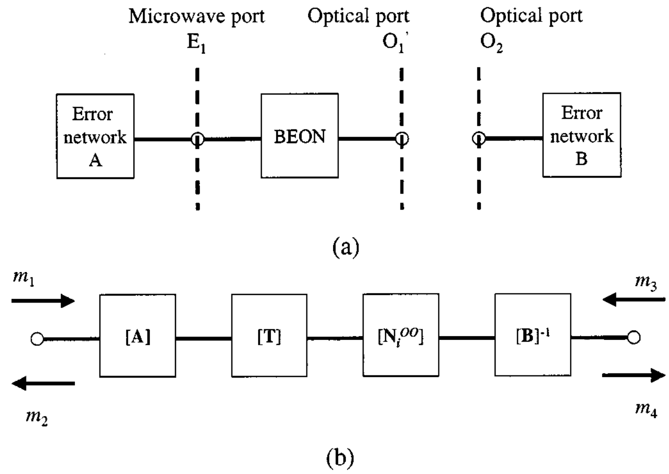

Fig. 5. (a) Measurement configuration for the combined E/O and O/E two-tier calibration. (b) Corresponding calibration model.

where m_1, m_2, m_3, m_4 are the measured power waves at the detectors, as shown schematically in Fig. 5(b), and $[\mathbf{M}]$ is the matrix product

$$[\mathbf{M}] = \begin{pmatrix} m_1' & m_3'' \\ m_2' & m_2'' \end{pmatrix} \begin{pmatrix} m_3' & m_3'' \\ m_4' & m_4'' \end{pmatrix}^{-1}$$

where the single and double primes represent the forward and reverse directions. $\mathbf{T}_{\mathrm{BEON}}^{\mathrm{EO}}$ is the T-matrix of the BEON and N_i^{OO} are the T-matrices of the optical standards.

The $\mathrm{T}xy$ calibration procedure will see an effective error network at O_1', which is the cascade of error network A and the BEON, i.e., the BEON is treated as an integral part of the BLNA. Hence, the calibration equations can be rewritten as

$$\mathbf{M}_1 = \mathbf{A}_{\mathrm{eff}}\mathbf{N}_1^{\mathrm{OO}}\mathbf{B}^{-1} \tag{4}$$

$$\mathbf{M}_2' = m_{2x}\mathbf{A}_{\mathrm{eff}}\mathbf{N}_2^{\mathrm{OO}}\mathbf{B}^{-1} \tag{5}$$

and

$$\mathbf{M}_3' = m_{3x}\mathbf{A}_{\mathrm{eff}}\mathbf{N}_3^{\mathrm{OO}}\mathbf{B}^{-1} \tag{6}$$

where

$$\mathbf{A}_{\mathrm{eff}} = \mathbf{A}\mathbf{T}_{\mathrm{BEON}}^{\mathrm{EO}}. \tag{7}$$

Therefore, if the $\mathrm{T}xy$ procedure is followed as in [8], the normalized matrix $\overline{\mathbf{A}_{\mathrm{eff}}}$ can be evaluated where the bar indicates normalization. In addition, for the E/O calibration, the effect of the BEON has to be finally deembedded from $\overline{\mathbf{A}_{\mathrm{eff}}}$ because the BEON is not used as part of the BLNA for subsequent measurements. Starting with the equality

$$\overline{\mathbf{A}_{\mathrm{eff}}} = \overline{\mathbf{A}\mathbf{T}_{\mathrm{BEON}}^{\mathrm{EO}}} \tag{8}$$

the constant factor, which is required to obtain $\overline{\mathbf{A}_{\mathrm{eff}}}$ from the product of $\mathbf{A}$ and $\mathbf{T}_{\mathrm{BEON}}^{\mathrm{EO}}$, can be lumped with one of these two matrices, i.e.,

$$\overline{\mathbf{A}_{\mathrm{eff}}} = \overline{\mathbf{A}}\mathbf{T}_{\mathrm{BEON}}^{\mathrm{EO}}. \tag{9}$$

Therefore,

$$\overline{\mathbf{A}} = \overline{\mathbf{A}_{\mathrm{eff}}}\mathbf{T}_{\mathrm{BEON}}^{\mathrm{EO}\,-1}. \tag{10}$$

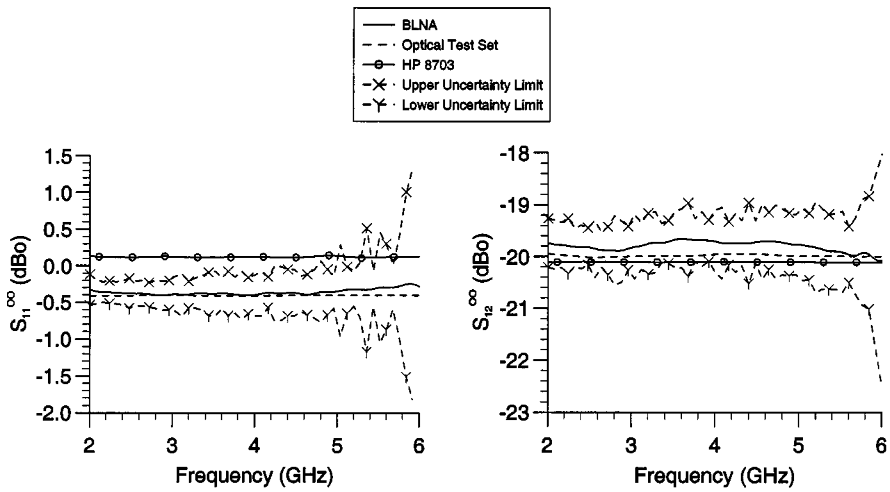

(a) (b)

Fig. 6. Calibrated optical magnitude measurements by the BLNA compared with the those by HP 8703A. (a) S_{11}^{OO} of a -0.2–dB reflect at Port 1. (b) S_{12}^{OO} of a -20–dB attenuator.

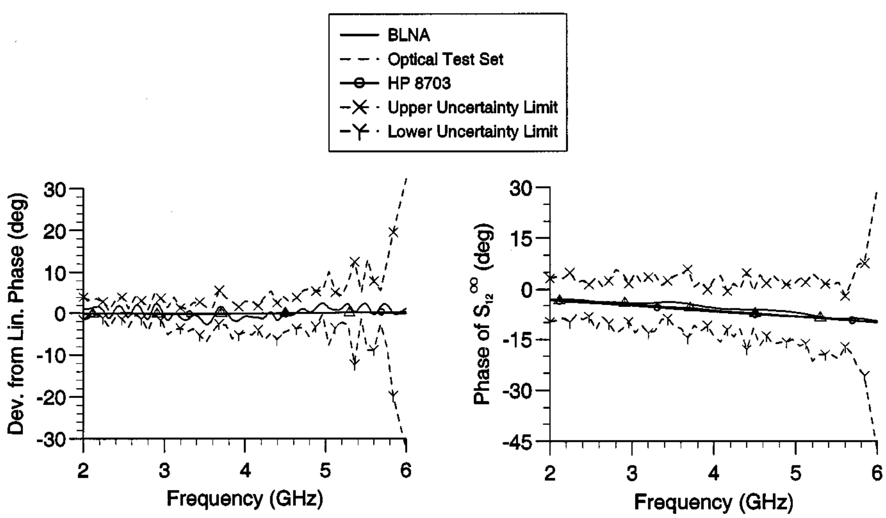

(a) (b)

Fig. 7. Calibrated optical phase measurements by the BLNA compared with those by the HP 8703A. (a) Deviation from linear phase of S_{11}^{OO} of a -0.2–dB reflect at the end of a length of fiber at Port 1. (b) Phase of S_{12}^{OO} of a -20–dB attenuator.

Thus, by treating the BEON as a black box whose S-parameters are pre-measured, it is possible to remove its response from this composite error network by a second-tier procedure to obtain a normalized version of the error network A. The matrix $\overline{\mathbf{B}}$ associated with error network B can be evaluated as in [8].

V. Experimental Results

A program on an instrumentation computer was written to control the BLNA. The program performs microwave, optical, and combined E/O and O/E $\mathrm{T}xy$ calibrations, and provides error-corrected measurements of all four types of lightwave components. The measured microwave results have been compared with the factory measured data, while the optical, O/E, and E/O measurements have been compared with results obtained using the HP 8703A lightwave analyzer.

Measurement of microwave verification standards were in excellent agreement with the factory measured data, and were also within the specified uncertainty limits. The major modifications to the HP 8510 microwave test set to configure the BLNA are the addition of a three-way switch in the source path, and the addition of power combiners in the sampler paths. The results show that the modifications have not affected the accuracy of the E/E measurements with the test set.

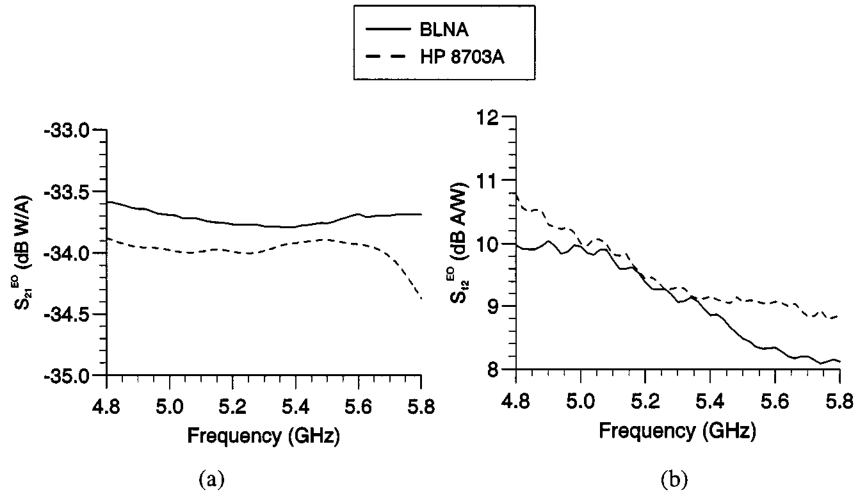

Fig. 8. Calibrated E/O and O/E measurements by the BLNA compared with those by HP 8703A. (a) $S_{21}^{\rm EO}$ of the BEON. (b) $S_{12}^{\rm EO}$ of the BEON.

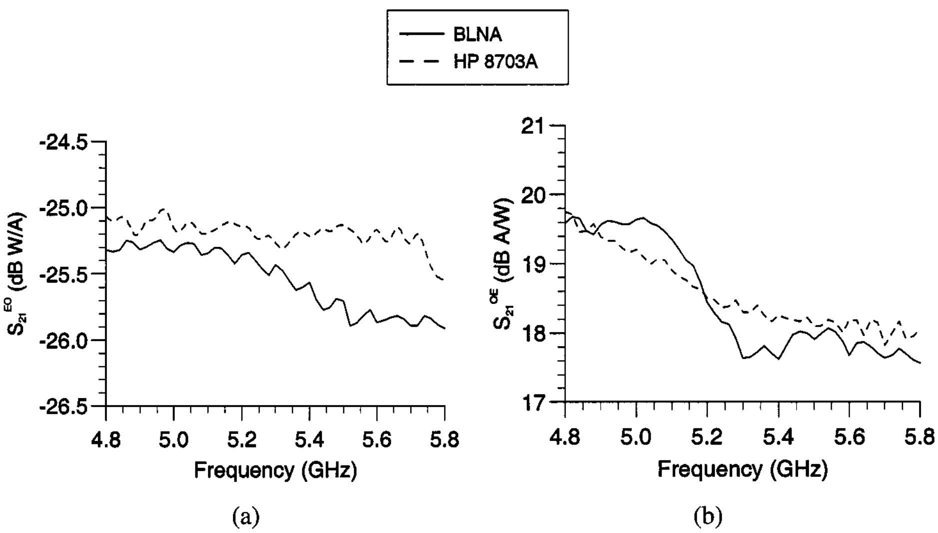

Fig. 9. Calibrated E/O and O/E measurements by the BLNA compared with the those by HP 8703A. (a) $S_{21}^{\rm EO}$ of the Ortel 3541B Laser. (b) $S_{21}^{\rm OE}$ of an HP amplified lightwave receiver.

A. Optical Measurements

The BLNA was calibrated between its optical ports using the thru-attenuate-reflect (TAR) routine [15]. This is found to be the best O/O calibration technique from the $\mathrm{T}xy$ family, both in terms of giving the most accurate broad-band results and not requiring index matching gel [16]. Optical magnitude measurements are shown in Fig. 6. It is evident that the results from the BLNA are within the limits of uncertainty from those of the optical test set in [12]. The measurement results from the HP 8703A are also within the uncertainty limits for transmission magnitude, but the improved reflection magnitude clearly shows the enhanced accuracy of the BLNA. Optical phase measurements are shown in Fig. 7. The results for both the optical reflection and transmission phase are well within the predicted uncertainty limits, which are calculated using the method in [18].

The apparently noisy results from the BLNA are probably due to two factors. Firstly, the use of a directly modulated laser reduced the power levels at the lightwave receivers. This increases the effect of the low-level noise of the receiver on the detected signals. Secondly, the unamplified receiver (which should ideally be followed by a low-noise amplifier) is followed by a power amplifier in the prototype, which also increases the signal noise content. These factors are observed to increase the noise floor by approximately 10 dBo. The use of an external modulator and amplified receivers throughout will reduce the noise effects.

B. E/O and O/E Measurements

The E/O and O/E measurements are performed after calibrating the analyzer with the two-tier calibration. The calibration standards used in the first-tier are an optical thru (T), optical

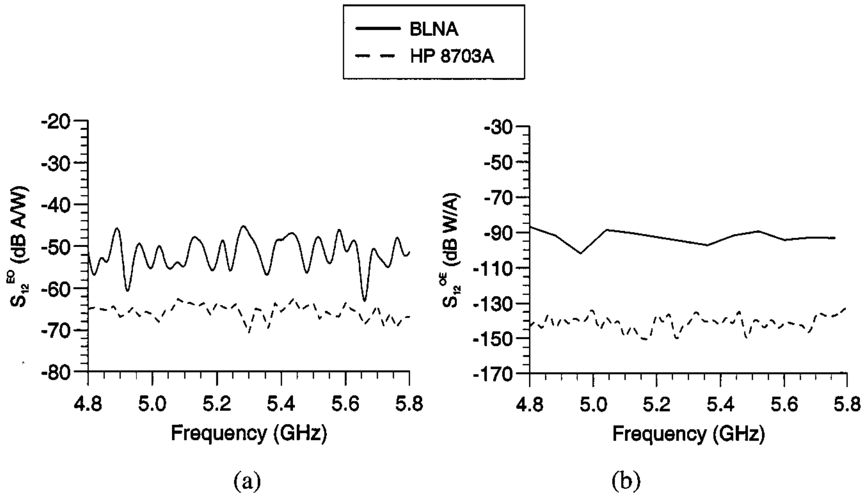

Fig. 10. Calibrated E/O and O/E noise floor measurements by the BLNA compared with the those by HP 8703A. (a) $S_{12}^{\rm EO}$. (b) $S_{12}^{\rm OE}$.

attenuator (A), and optical mirrors (R) cascaded in turn with the BEON. The BEON is identical to the one constructed in [13]. Deembedding of the BEON is then performed to obtain the E/O and O/E calibration coefficients. The BEON is remeasured after the calibration, and compared with the values used for the deembedding. It is evident that there is a good agreement between the two (Fig. 8).

Fig. 9 shows the measurement results of the forward transmission S-parameters of a laser (Ortel 3541B DFB) and a lightwave receiver. It is seen that the measurements with the HP 8703A and BLNA follow each other closely over most of the frequency range. Uncertainty limits similar to the microwave and optical cases are not presented since the method described in [18] cannot be applied to E/O and O/E cases.

Fig. 10 shows the reverse transmission S-parameters of the same components. It is essentially a noise-floor measurement because these two devices are unilateral. The noise floor obtained with the prototype BLNA is worse than the commercial analyzer, only because it employed a directly modulated laser and unamplified receiver.

VI. Conclusions

In this paper, a BLNA has been designed and demonstrated. The major advantages of the proposed BLNA over the present state-of-the-art commercial lightwave analyzer are its improved accuracy and capability to perform two-port S-parameter measurements of all four types of lightwave components without the need for connections and disconnections. Consequently, two-port self calibrations can be applied to both E/E and O/O components and both E/O and O/E components are measured between the same pair of ports of the BLNA. This allows the implementation of a combined E/O and O/E calibration. A novel two-tier combined E/O and O/E calibration has been proposed for this purpose. The generalized $\mathrm{T}xy$ self-calibration procedure is used in the first tier, and a deembedding procedure is used in the second tier to remove the effect of the BEON.

The prototype has provided results that closely follow the predicted values for both microwave and optical measurements. Its accuracy for optical reflection magnitude measurements is much better than those obtained with an existing commercial lightwave network analyzer. The E/O and O/E transmission measurements from both the commercial instrument and the BLNA show good agreement over most of the frequency range. The dynamic range reduction and the variations in the results with the prototype BLNA will be readily alleviated with the use of purpose-built hardware.

References

[1] L. Kazovsky, S. Benedetto, and A. Willner, *Optical Fiber Communication Systems*. Norwood, MA: Artech House, 1996.

[2] C. Lim, A. Nirmalathas, D. Novak, R. Waterhouse, and K. Ghorbani, “Full-duplex broadband fiber-wireless system incorporating baseband data transmission and a novel dispersion tolerant modulation scheme,” in *IEEE MTT-S Int. Microwave Symp. Dig.*, vol. 3, Anaheim, CA, June 13–19, 1999, pp. 1201–1204.

[3] R. D. Esman, M. Y. Frankel, and P. J. Matthews, “New array capabilities by photonic beamforming,” in *IEEE MTT-S Int. Microwave Symp. Dig.*, vol. 3, Baltimore, MD, June 7–12, 1998, pp. 1363–1366.

[4] T. A. Cusick, S. Iezekiel, R. E. Miles, S. Sales, and J. Capmany, “Synthesis of all-optical microwave filters using Mach–Zehnder lattices,” *IEEE Trans. Microwave Theory Tech.*, vol. 45, pp. 1458–1462, Aug. 1997.

[5] A. J. Seeds and A. A. A. Salles, “Optical control of microwave semiconductor devices,” *IEEE Trans. Microwave Theory Tech.*, vol. 38, pp. 577–585, May 1990.

[6] D. K. Rytting, “Analysis of error correction techniques,” in *Hewlett-Packard RF Microwave Measurement Symp. Exhibition*, Mar. 1982.

[7] R. B. Marks and K. Phillips, “Wafer-level ANA calibrations at NIST,” in *36th ARFTG Conf. Dig.*, Dec. 1989, pp. 11–24.

[8] H. Heuermann and B. Schiek, “Robust algorithms for Txx network analyzer self-calibration procedures,” *IEEE Trans. Instrum. Meas.*, vol. 43, pp. 18–23, Feb. 1994.

[9] R. W. Wong, P. R. Hernday, and D. R. Harkins, “High-speed lightwave component analysis to 20 GHz,” *Hewlett-Packard J.*, vol. 42, no. 1, pp. 6–13, Feb. 1991.

[10] D. D. Curtis and E. E. Ames, “Optical test set for microwave fiber-optic network analysis,” *IEEE Trans. Microwave Theory Tech.*, vol. 38, pp. 552–559, May 1990.

[11] D. R. Harkins and M. A. Heinzelman, “Accuracy considerations and error correction techniques for 20 GHz lightwave component analysis,” *Hewlett-Packard J.*, vol. 42, no. 1, pp. 34–40, Feb. 1991.

[12] S. Iezekiel, C. M. Snowden, and M. J. Howes, "Scattering parameter characterization of microwave optoelectronic devices and fiber-optic networks," *IEEE Microwave Guided Wave Lett.*, vol. 1, no. 9, pp. 233–235, Sept. 1991.
[13] B. Elamaran, R. D. Pollard, and S. Iezekiel, "Simulation and implementation of lightwave component characterization using a bilateral electro-optic network," *IEEE Trans. Microwave Theory Tech.*, vol. 45, pp. 1493–1496, Aug. 1997.
[14] A. H. Quoc and S. Tedjini, "Measurement & calibration procedure for the characterization of the scattering parameters in microwave fiber-optic devices," in *Proc. 24th European Microwave Conf.*, Nice, France, 1994, pp. 934–939.
[15] B. Elamaran, R. D. Pollard, and S. Iezekiel, "$\mathrm{Ta}x$ calibration of optical scattering parameter test set," in *Int. Microwave Photon. Symp. Dig.*, Princeton, NJ, Oct. 1998, pp. 55–58.
[16] ——, "Optical domain implementation of the microwave $\mathrm{T}xy$ family of calibration techniques," *IEEE Trans. Microwave Theory Tech.*, vol. 47, pp. 1373–1380, July 1999.
[17] ——, "Implementation and calibration of a two-port electro-optic network analyzer," *IEEE Microwave Guided Wave Lett.*, vol. 9, pp. 369–371, Sept. 1999.
[18] B. Donecker, "Determining the measurement accuracy of the HP 8510 microwave network analyzer," in *Hewlett-Packard RF Microwave Measurement Symp. Exhibition*, Mar. 1985.

Balasundaram Elamaran (S'94–M'99) was born in Jaffna, Sri Lanka, in 1974. He received the B.Eng. (with honours) and Ph.D. degrees from The University of Leeds, Leeds, U.K., in 1995 and 1999, respectively.

In March 2000, he joined the Lightwave Division, Agilent Technologies, Santa Rosa, CA, as a Research and Development Hardware Design Engineer. His current research interests are in the areas of microwave photonic instrumentation and microwave and millimeter-wave circuit design. He was previously a Post-Doctoral Research Fellow at the University of Hawaii at Manoa, where his research was in the areas of self-oscillating mixers and beam-steering antenna designs.

Dr. Elamaran was the recipient of the 1998 IEEE Microwave Theory and Techniques Society (IEEE MTT-S) Graduate Fellowship and the 1999 Institution of Electrical Engineers Wheatstone Measurement Prize.

Roger D. Pollard (M'77–SM'91–F'97) was born in London, U.K., in 1946. He received the B.Sc. and Ph.D. in electrical and electronic engineering from The University of Leeds, Leeds, U.K.

He currently holds the Agilent Technologies Chair in High Frequency Measurements and is Head of the School of Electronic and Electrical Engineering, The University of Leeds, where he has been a faculty member since 1974. He is an active member of the Institute of Microwaves and Photonics (one of the constituent parts of the school), which has over 40 active researchers, a strong graduate program, and has made contributions to microwave passive and active device research. The activity has significant industrial collaboration as well as a presence in continuing education. His personal research interests are in microwave network measurements, calibration and error correction, microwave and millimeter-wave circuits, terahertz technology, and large-signal and nonlinear characterization. He has been a consultant to Agilent Technologies (previously Hewlett-Packard Company), Santa Rosa, CA, since 1981. He has authored or co-authored over 100 technical papers and holds three patents.

Dr. Pollard is a Chartered Engineer and a member of the Institution of Electrical Engineers (IEE), U.K. He is an Editorial Board member of IEEE TRANSACTIONS ON MICROWAVE THEORY AND TECHNIQUES and has been on the Technical Program Committee for the IEEE Microwave Theory and Techniques Society (IEEE MTT-S) International Microwave Symposium since 1986. He is and active IEEE volunteer, as an elected member of the Administrative Committee and 1998 President of the IEEE MTT-S and currently chair of IEEE's Electronic Products Committee. He is also an editor for the IEEE Press book series on *RF & Microwave Technology*.

Stavros Iezekiel (S'88–M'90–SM'00) was born in Coventry, U.K., in 1966. He received the B.Eng. and Ph.D. degrees from The University of Leeds, Leeds, U.K., in 1987 and 1991, respectively.

From 1991 to 1993, he worked in conjunction with the M/A-COM Corporate Research and Development Center on the development of microwave photonic multichip modules. Since 1993, he has been a Lecturer in high-frequency analog electronics at The University of Leeds, where he leads the research activity in microwave photonics.

Dr. Iezekiel is a member of the UKRI MTT-S/Electron Devices Society (ED-S)/Antennas and Propagation Society (AP-S)/Lasers and Electro-Optics Society (LEOS) Joint Chapter AdCom. He has organized a number of IEEE events and is also the membership development officer for the IEEE UKRI Section. He was the recipient of the 1999 Institution of Electrical Engineers (IEE) Measurement Prize for his work on lightwave network analysis.